

### §30. Magnetic Configuration Study of $L = 1$ Helical Axis Heliotron

Yokoyama, M.,  
Nakamura, Y., Wakatani, M. (Graduate School of Energy Science, Kyoto U.),  
Isaev, M. Yu., Shafranov, V.D. (Kurchatov Inst.),  
Cooper, W.A. (Confédération Suisse, Ecole Polytechnique Fédérale de Lausanne)

The helical axis heliotron device, Heliotron J (H-J), has been proposed at Kyoto University. In order to keep the experimental flexibility, the  $L = 1/M = 4$  continuous helical coil (HC) has been chosen. Recent studies have shown the significant roles of the bumpy field for collisionless particle confinement and bootstrap current. The bumpy field was not present in planar axis heliotrons. There are two sets of toroidal coils (TC-A,B) with different coil current. This current modulation is effective to control the bumpy field in a wide range. Three pairs of poloidal coils (PC) also have been proposed for further flexibility. The set of PC (PC-OV) used in the Heliotron E is usable to generate a uniform vertical field. In addition, two sets of PC have been proposed. Example positions are  $(R, Z) = (1.7, \pm 0.78)$  m (PC-AV) and  $(R, Z) = (0.45, 0)$  m (PC-IV).

The following parameters are fixed. (1)  $B_t(1.2\text{m})/B_h(1.2\text{m}) = 1.5$ , where  $B_t(B_h)$  is the toroidal field strength by TC (HC). (2)  $I_{TA}/I_{TB} = 5/2$ , where  $I_{TA}(I_{TB})$  is the current in TC-A (TC-B). (3) PC-OV current is 0.84 MA in the opposite direction to HC current with 0.96 MA.

Principal properties are compared among four configurations with different characteristics.

- 201:**  $(I_{AV}, I_{IV}) = (0.0, 0.0)$ ,  $\langle R_{ax} \rangle \sim R_0$ .
- 203:**  $(I_{AV}, I_{IV}) = (0.0, 0.7)$ ,  $\langle R_{ax} \rangle < R_0$ , high  $B_{10}/(a/\langle R_{ax} \rangle)$ , keeping the magnetic well even when  $\langle R_{ax} \rangle < R_0$ .
- 207:**  $(I_{AV}, I_{IV}) = (0.0, -1.0)$ ,  $\langle R_{ax} \rangle > R_0$ ,  $B_{10}/(a/\langle R_{ax} \rangle) \sim 1$ , unclosed  $B_{min}$  contours.
- 212:**  $(I_{AV}, I_{IV}) = (0.16, 1.0)$ ,  $\langle R_{ax} \rangle > R_0$ , unclosed  $B_{min}$  contours, deeper magnetic well, higher  $t$ .

The ratios,  $B_{10}/B_{11}$  and  $B_{01}/B_{11}$  (at  $r/a = 0.5$ ), are summarized in Table I. Here,  $B_{11}$  and  $B_{01}$  denote the principal helicity and bumpiness. The

importance of negative  $B_{01}/B_{11}$  for improving the particle confinement has been clarified. This ratio becomes more negative as  $\langle R_{ax} \rangle$  is reduced with more positive  $I_{IV}$ . Based on this favorable ratio of  $B_{01}/B_{11}$ ,  $B_{min}$  contours tend to close for this region of  $I_{IV}$ . However, when  $I_{AV}$  is positive,  $\langle R_{ax} \rangle$  becomes larger and  $B_{min}$  contours become open (cf., comparison between 203 and 212). In this case, active control of bumpy field with TC through  $I_{TA}/I_{TB}$  would be required.

Collisionless particle confinement is studied. The protons are launched from  $r/a = 0.25, 0.5, 0.75$  with assumed temperature profile:  $T(r) = 1.0[1 - (r/a)^2]$  [keV]. The loss rate for configurations 201 and 207 is 12.6% and 24.2%. The collisionless particle confinement improves as  $B_{01}/B_{11}$  becomes almost zero to negative, reflecting the closure of  $B_{min}$  contours.

The DKES code has been utilized to evaluate the neoclassical transport properties. They are calculated at the magnetic surface with  $|B_{10}| = 0.1$ . Figure 1(a) shows the monoenergetic particle diffusion coefficient and 1(b) the bootstrap coefficient, where  $\nu_*$  denotes the effective collision frequency. The  $1/\nu$  diffusivity reduces for configurations 201 and 203 with negative  $B_{01}/B_{11}$  compared to that for 207 and 212 with positive or almost zero  $B_{01}/B_{11}$ . The bootstrap coefficient also changes with  $B_{01}/B_{11}$ . Figures 1 imply flexibility in experiments for neoclassical transport properties through PC current variation.

Configuration	$B_{10}/B_{11}$	$B_{01}/B_{11}$
201	0.75	-0.65
203	0.88	-1.13
207	0.66	0.08
212	0.76	0.17

Tab. I The ratios,  $B_{10}/B_{11}$  and  $B_{01}/B_{11}$ , for configurations 201, 203, 207 and 212.

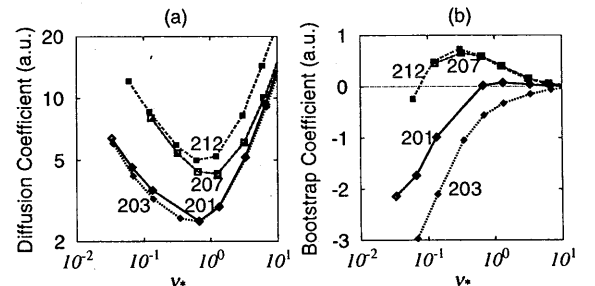


Fig. 1: (a) Neoclassical particle diffusivity and (b) bootstrap coefficient for configurations 201, 203, 207 and 212.